

RESEARCH LETTER

10.1002/2016GL070695

Key Points:

- Observed weaker decline of sulfate in DJF than in JJA in response to SO₂ emission controls in the U.S. is not well captured by CMIP5 models
- This seasonal contrast results from faster in-cloud oxidation of SO₂ by ozone, promoted by diminishing cloud acidity
- Anthropogenic ammonia indirectly reduces the effectiveness of SO₂ emission controls in decreasing sulfate in winter

Supporting Information:

- Supporting Information S1

Correspondence to:

F. Paulot,
Fabien.Paulot@noaa.gov

Citation:

Paulot, F., S. Fan, and L. W. Horowitz (2017), Contrasting seasonal responses of sulfate aerosols to declining SO₂ emissions in the Eastern U.S.: Implications for the efficacy of SO₂ emission controls, *Geophys. Res. Lett.*, *44*, 455–464, doi:10.1002/2016GL070695.

Received 2 AUG 2016

Accepted 27 OCT 2016

Accepted article online 31 OCT 2016

Published online 5 JAN 2017

Contrasting seasonal responses of sulfate aerosols to declining SO₂ emissions in the Eastern U.S.: Implications for the efficacy of SO₂ emission controls

F. Paulot^{1,2}, S. Fan¹, and L. W. Horowitz¹

¹Geophysical Fluid Dynamics Laboratory, National Oceanic and Atmospheric Administration, Princeton, New Jersey, USA,

²Program in Atmospheric and Oceanic Sciences, Princeton University, Princeton, New Jersey, USA

Abstract Stringent controls have reduced U.S. SO₂ emissions by over 60% since the late 1990s. These controls have been more effective at reducing surface [SO₄²⁻] in summer (June, July, and August) than in winter (December, January, and February (DJF)), a seasonal contrast that is not robustly captured by Climate Model Intercomparison Project 5 global models. We use the Geophysical Fluid Dynamics Laboratory AM3 chemistry-climate model to show that oxidant limitation during winter causes [SO₄²⁻] (DJF) to be sensitive to primary SO₄²⁻ emissions, in-cloud titration of H₂O₂, and in-cloud oxidation by O₃. The observed contrast in the seasonal response of [SO₄²⁻] to decreasing SO₂ emissions is best explained by the O₃ reaction, whose rate coefficient has increased over the past decades as a result of increasing NH₃ emissions and decreasing SO₂ emissions, both of which lower cloud water acidity. The fraction of SO₂ oxidized to SO₄²⁻ is projected to keep increasing in future decades, delaying improvements in wintertime air quality.

1. Introduction

Long-term observations in both the U.S. and Europe show that regulations aimed at curbing SO₂ emissions have successfully reduced the surface concentration of sulfate aerosols ([SO₄²⁻]) with major benefits for visibility [Mueller, 2003; Hand et al., 2014], air quality [Hand et al., 2012b], and acid rain [Garmo et al., 2014]. These observations also show that [SO₄²⁻] has declined less rapidly than SO₂ emissions, especially in winter [Manktelow et al., 2007; Hand et al., 2012a, 2012b; Tanner et al., 2015; Banzhaf et al., 2015]. In this study, we focus on the photochemical processes that induce these observed seasonal differences in the response of [SO₄²⁻] to decreasing SO₂ emissions.

SO₂ oxidation can proceed via the gas phase reaction with OH but is thought to be dominated by the in-cloud reaction of H₂O₂ with bisulfide (HSO₃⁻) [Seinfeld and Pandis, 2006]. This reaction is fast and largely insensitive to cloud acidity, such that the in-cloud oxidation of SO₂ is effectively limited by the availability of H₂O₂ [Seinfeld and Pandis, 2006; Ervens, 2015]. Manktelow et al. [2007] noted that the in-cloud titration of H₂O₂ by SO₂ is consistent with the sublinear response of [SO₄²⁻] to changes in SO₂ emissions, especially in winter when H₂O₂ production is lowest in the northern midlatitudes. In-cloud oxidation of SO₂ to SO₄²⁻ may also proceed via the reaction of O₃ with sulfide (SO₃²⁻). Unlike the oxidation by H₂O₂, this reaction exhibits a strong pH dependence, with the effective reaction rate coefficient ($k_{O_3}^{SO_2}$) increasing as 10^{pH} above pH = 4.5 [Seinfeld and Pandis, 2006]. The relative contribution of the O₃ pathway to SO₄²⁻ production remains uncertain, with model estimates ranging widely from 1% to 50% [Barth et al., 2000; Berglen et al., 2004; Alexander et al., 2009; Bellouin et al., 2011; Paulot et al., 2016]. In the 1990s, acid rain was prevalent and the oxidation of SO₂ by O₃ was often neglected in models of the sulfur cycle [Chin et al., 1996; Koch et al., 1999], an assumption supported by isotopic measurements [Alexander et al., 2009; Sofen et al., 2011]. In the last 10 years, cloud acidity has declined in the U.S. and Europe [Garmo et al., 2014] as a result of controls on NO_x and SO₂ emissions. Banzhaf et al. [2015] recently showed that the associated increase of $k_{O_3}^{SO_2}$ was an important contributor to the sublinear response of [SO₄²⁻] to SO₂ emission controls in Europe.

In this study, we first compare the observed change of [SO₄²⁻] in winter (December, January, and February (DJF)) and in summer (June, July, and August (JJA)) in the Eastern U.S. over the last 30 years with the SO₂

emission trend and the $[\text{SO}_4^{2-}]$ trend simulated by models from the Climate Model Intercomparison Project 5 (CMIP5). Second, we use the atmospheric chemistry-climate model (AM3) from the Geophysical Fluid Dynamics Laboratory (GFDL) to examine the photochemical processes that contribute to the weaker decline of $[\text{SO}_4^{2-}]$ in DJF relative to JJA. Finally, we discuss the indirect contribution of anthropogenic NH_3 emissions to challenges in reducing wintertime $[\text{SO}_4^{2-}]$.

2. Method

We use surface observations of $[\text{SO}_4^{2-}]$ from the Clean Air Status and Trend Network (CASTNET). CASTNET was established under the 1991 Clean Air Act Amendments to monitor changes in air quality associated with emission control programs. Total SO_4^{2-} (TSO4) is collected weekly on filters 10 m above ground at over 100 sites [Malm *et al.*, 2002]. Comparisons against independent measurement techniques suggest that CASTNET TSO4 has no significant bias [Ames and Malm, 2001; Malm *et al.*, 2002]. We obtain seasonally averaged TSO4 (DJF) and TSO4 (JJA) from the U.S. Environmental Protection Agency (EPA, <https://www.epa.gov/castnet>). For a seasonal mean to be valid, the U.S. EPA requires at least 75% of the measurements over this season to pass quality controls. We focus our analysis on the Eastern U.S., where $[\text{SO}_4^{2-}]$ has historically been most elevated [Hand *et al.*, 2012b].

We use simulated surface $[\text{SO}_4^{2-}]$ from 11 global models that participated in CMIP5 and reported $[\text{SO}_4^{2-}]$ [Taylor *et al.*, 2012; Flato *et al.*, 2013; Collins *et al.*, 2013]. These models include a comprehensive representation of SO_2 gas phase and aqueous oxidation [Flato *et al.*, 2013]. We consider the model response of $[\text{SO}_4^{2-}]$ (DJF) and $[\text{SO}_4^{2-}]$ (JJA) to declining SO_2 emissions over both the historical period (1985–2005) and the RCP4.5 scenario (2005–2050). For models reporting several realizations over both periods, we consider the mean surface $[\text{SO}_4^{2-}]$ across these realizations (see Table S1 in the supporting information).

We perform additional simulations with the GFDL-AM3 model [Donner *et al.*, 2011; Naik *et al.*, 2013], the atmospheric chemistry-climate component of the GFDL-CM3 model [Donner *et al.*, 2011; Griffies *et al.*, 2011; John *et al.*, 2012], with revisions to the treatment of SO_4^{2-} chemistry and wet deposition as described in Paulot *et al.* [2016]. Anthropogenic emissions are identical to those used in CMIP5 models [Lamarque *et al.*, 2011; Meinshausen *et al.*, 2011; Thomson *et al.*, 2011; van Vuuren *et al.*, 2011] except for NH_3 to which we apply monthly variations from HTAPv2 [Janssens-Maenhout *et al.*, 2015]. In AM3, SO_4^{2-} is produced through the oxidation of SO_2 in the gas phase by OH, in liquid cloud by H_2O_2 and O_3 , in precipitation by H_2O_2 , and by heterogeneous reaction on dust particles [Paulot *et al.*, 2016]. Cloud pH is calculated iteratively based on the in-cloud concentrations of gases (NH_3 , HNO_3 , SO_2 , CO_2 , HCOOH , and CH_3COOH) and aerosols (NH_4^+ , NO_3^- , and SO_4^{2-}). Seventy percent of aerosols are assumed to be dissolved in liquid clouds, while the solubility of gases reflects their effective Henry's law constants. To quantify the impact of cloud pH on SO_4^{2-} production, we perform three additional simulations: with prescribed cloud pH = 5 (AM3_pH5), without anthropogenic emissions of NH_3 (AM3_NA), and without seasonality for anthropogenic NH_3 emissions (AM3_NS), similar to the emissions used in CMIP5. A further simulation considers the impact of transition metal chemistry following Alexander *et al.* [2009] (AM3_TM; see supporting information for details). Anthropogenic S is emitted entirely as SO_2 , except in AM3_TM where 3% is emitted as SO_4^{2-} [Chin *et al.*, 2000]. Each simulation is performed in two segments. First, from 1985 to 2014, the model horizontal winds are nudged to 6-hourly horizontal winds from the National Centers for Environmental Prediction reanalysis [Kalnay *et al.*, 1996; Lin *et al.*, 2012] and observed sea surface temperature (SST) and sea ice cover (SIC) are used [Rayner *et al.*, 2003]. Second, from 2015 to 2050, no nudging is performed and we use 1980–2000 climatological monthly mean SST and SIC [Rayner *et al.*, 2003]. The contributions of the different oxidation pathways to SO_4^{2-} production for each configuration in 2005 are provided in Table S2. Differences in simulated $[\text{SO}_4^{2-}]$ across configurations are dominated by photochemistry especially in the first segment, as nudging results in similar circulation, precipitation, and other climate variables. Nudging also facilitates comparison with observations.

3. Results and Discussion

3.1. Relative Trends of $[\text{SO}_4^{2-}]$ in Winter and Summer From Observations and CMIP5 Model Simulations

Figure 1 shows observed and simulated $[\text{SO}_4^{2-}]$ in JJA and DJF at Shenandoah National Park (38.5°N, –78.4°E) from 1990 to 2014. The average model bias is +20% in winter and –20% in summer, but seasonal biases can exceed 100% for individual models, which could reflect errors in SO_2 and SO_4^{2-} deposition, SO_2 photochemistry, and SO_2 emissions [Ervens, 2015]. For instance, we recently showed that the large positive bias in summer

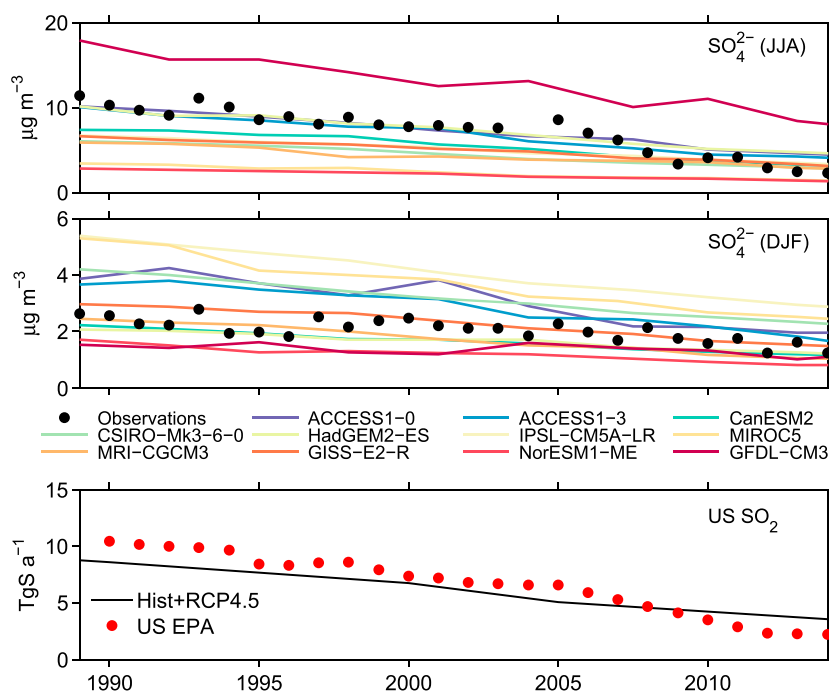


Figure 1. Observed and simulated changes in $[\text{SO}_4^{2-}]$ at Shenandoah National Park in summer (top) and winter (middle). Anthropogenic U.S. SO_2 emissions from the U.S. EPA National Emission Inventory [EPA, 2016] and the CMIP5 inventory are shown in the bottom panel. For readability, the model outputs are binned over 3 consecutive years.

(+80%) and negative bias in winter (−30%) in GFDL-CM3 stemmed from a poor representation of wet deposition [Paulot et al., 2016]. Observations show that $[\text{SO}_4^{2-}]$ has decreased by $10\% \text{ a}^{-1}$, similar to the trend in U.S. SO_2 emissions [U.S. Environmental Protection Agency (U.S. EPA), 2016], while $[\text{SO}_4^{2-}]$ in DJF has declined by only $5\% \text{ a}^{-1}$. Over the same period, simulated $[\text{SO}_4^{2-}]$ (JJA) and $[\text{SO}_4^{2-}]$ (DJF) have decreased by $3.4 \pm 0.4\% \text{ a}^{-1}$ and $2.8 \pm 0.7\% \text{ a}^{-1}$, respectively, underestimating the observed trend and failing to capture its large seasonality. The underestimate of the $[\text{SO}_4^{2-}]$ decline is consistent with the weaker decline of SO_2 emissions in the RCP4.5 scenario over the 2000–2014 period relative to the U.S. EPA National Emission Inventory (Figure 1, bottom). In subsequent analysis, we focus on change in the ratio of winter to summer $[\text{SO}_4^{2-}]$ (R_{ws}), as this metric allows us to better isolate changes in SO_2 photochemistry from biases in wet deposition or SO_2 emissions, whose seasonalities are unlikely to have changed significantly.

Figure 2 shows that R_{ws} increases at all CASTNET stations over the 1985–2015 period, similar to Shenandoah. The value of R_{ws} varies spatially. It is highest in the Midwest (where it exceeds 1 in Wisconsin) and lowest near large sources of SO_2 (e.g., Ohio Valley).

Figure 3 shows the evolution of the observed ratio of R_{ws} as a function of $[\text{SO}_4^{2-}]$ (JJA) at nine stations located from the Midwest to the Atlantic Coast (red stars in Figure 2) with at least 15 years of both winter and summer TSO4 observations. At all sites, we find a significant negative correlation ($p < 0.01$) between $[\text{SO}_4^{2-}]$ (JJA) and R_{ws} , indicating that R_{ws} increases while $[\text{SO}_4^{2-}]$ (JJA) declines. Over the same period, four models CanESM2 [Lohmann et al., 1999; von Salzen et al., 2000; Salzen et al., 2013], HadGEM2-ES [Collins et al., 2011], IPSL-CM5A-LR [Dufresne et al., 2013], and GFDL-CM3 [Donner et al., 2011] also show a significant negative correlation between $[\text{SO}_4^{2-}]$ (JJA) and R_{ws} at all sites (Table S3). GISS-E2-R [Schmidt et al., 2006; Shindell et al., 2013] also qualitatively captures the relationship between R_{ws} and $[\text{SO}_4^{2-}]$ (JJA) when considering the extended 1985–2050 period. The other six models ACCESS1-0 [Dix et al., 2013], ACCESS1-3 [Dix et al., 2013], CSIRO-Mk3-6-0 [Rotstajn and Lohmann, 2002; Rotstajn et al., 2012], MIROC5 [Takemura et al., 2005; Watanabe et al., 2010], MRI-CGCM3 [Yukimoto et al., 2012], and NorESM1-ME [Kirkevåg et al., 2013; Bentsen et al., 2013] show no significant change or an increase of R_{ws} at some sites as $[\text{SO}_4^{2-}]$ (JJA) declines (Table S3). Interestingly, there is no clear link between the ability of models to qualitatively capture the relationship between R_{ws} and $[\text{SO}_4^{2-}]$ (JJA) and the model bias for $[\text{SO}_4^{2-}]$ (DJF) and $[\text{SO}_4^{2-}]$ (JJA) individually.

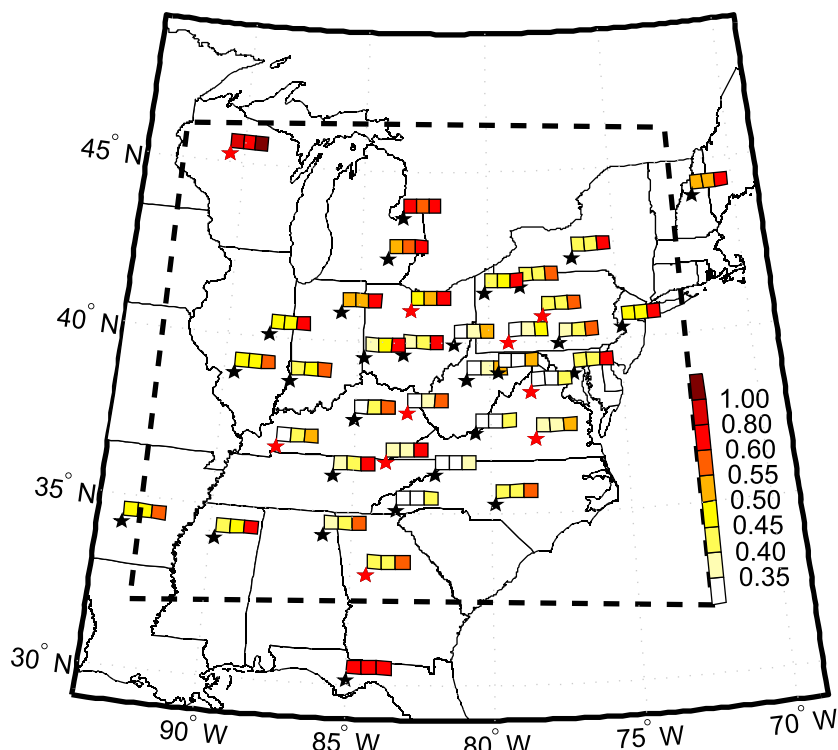


Figure 2. Observed ratio (R_{ws}) of $[SO_4^{2-}]$ in DJF to $[SO_4^{2-}]$ in JJA at CASTNET sites. For each site (star), the three squares denote the mean R_{ws} from 1985 to 1994 (left square), 1995 to 2004 (middle square), and 2006 to 2014 (right square). Red stars highlight the locations of the sites shown in Figures 3 and 4.

3.2. Impact of Cloud pH on $[SO_4^{2-}]$ (DJF)

Figure 4 shows the simulated relationship between $[SO_4^{2-}]$ (JJA) and R_{ws} in the different AM3 configurations described earlier. From 1985 to 2015, AM3_BASE simulates a significant negative correlation between $[SO_4^{2-}]$ (JJA) and R_{ws} at all sites, while AM3_pH5 exhibits no significant change in R_{ws} at seven sites. However, AM3_pH5 shows a lower bias in R_{ws} than in AM3_BASE. These two configurations of AM3 qualitatively capture the range of relationships between $[SO_4^{2-}]$ (JJA) and R_{ws} across CMIP5 models, suggesting that differences in the representation of cloud pH contribute to model diversity.

Figure 5 shows the winter and summer conversion efficiency (η) of SO_2 to SO_4^{2-} in the Eastern U.S. (Figure 2) as a function of the total source of SO_2 over the 1985–2050 period. We define η as follows:

$$\eta = \frac{P(SO_4^{2-})}{S(SO_2)} \quad (1)$$

where $P(SO_4^{2-})$ is the photochemical production of SO_4^{2-} and $S(SO_2)$ is the total source of SO_2 (i.e., emissions, photochemical production, and import). Note that emissions of primary SO_4^{2-} (in AM3_TM) are included in both $P(SO_4^{2-})$ and $S(SO_2)$. In summer, $P(SO_4^{2-})$ is dominated by the oxidation of SO_2 by H_2O_2 and OH. η_{JJA} is comparable across experiments and increases little as $S(SO_2)$ decreases by more than an order of magnitude. In contrast, η_{DJF} increases from 5% to 50% in AM3_BASE and from 20 to 35% in AM3_pH5. As the lifetime of SO_4^{2-} changes little over the 1985–2050 period, the increase of R_{ws} with decreasing $[SO_4^{2-}]$ (JJA) in our model reflects the increase of η_{DJF} with decreasing $S(SO_2)$.

The simulated evolution of η_{DJF} with diminishing $S(SO_2)$ in AM3_BASE exhibits two distinct regimes. First, in the 1990s, during which SO_2 oxidation is dominated by H_2O_2 , the increase of η_{DJF} reflects the reduced titration of H_2O_2 in clouds (regime 1). Second, from 2000 onward, η_{DJF} increases more rapidly, driven by greater oxidation of SO_2 by O_3 (regime 2). This increase is driven by diminishing cloud acidity (reflected by increasing rain pH, e.g., <http://nadp.sws.uiuc.edu>), which increases $k_{O_3}^{SO_2}$ and allows faster oxidation of SO_2 by O_3 . By 2020, the oxidation of SO_2 by O_3 is projected to be the largest source of SO_4^{2-} in winter.

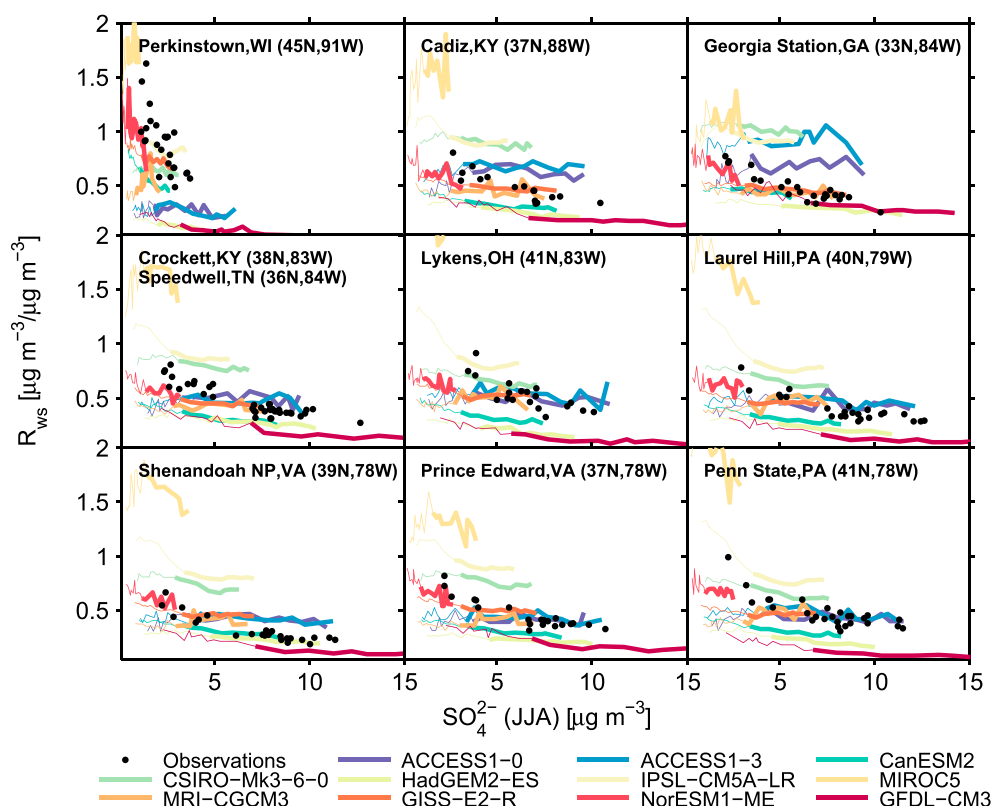


Figure 3. Observed (black) and simulated relationship between $[\text{SO}_4^{2-}]$ (JJA) and the ratio of $[\text{SO}_4^{2-}]$ (DJF) to $[\text{SO}_4^{2-}]$ (JJA) (R_{ws}). Observations are from the U.S. EPA CASTNET network from 1985 to 2014 (see red stars in Figure 2 for the locations of the stations). Simulated surface $[\text{SO}_4^{2-}]$ from the different CMIP5 models is sampled at the location of the CASTNET sites from 1985 to 2050. For readability, the model outputs are binned over 3 consecutive $[\text{SO}_4^{2-}]$ (JJA). Thick lines denote the CMIP5 model results over the 1985–2015 period.

The existence of two photochemical regimes for winter SO_4^{2-} production helps explain the steeper increase of R_{ws} with decreasing $[\text{SO}_4^{2-}]$ (JJA) at Perkinstown (WI) than at other stations (Figure 3). Perkinstown (WI) is located in the U.S. Midwest, where cloud acidity is lower than in the Eastern U.S. due to large agricultural sources of NH_3 and low combustion sources (see <http://nadp.sws.uiuc.edu> for rain pH). The larger derivative of R_{ws} with respect to $[\text{SO}_4^{2-}]$ (JJA) at this site suggests that O_3 makes an important contribution to SO_2 oxidation in this region (regime 2). Indeed, we find that AM3_BASE captures this geographical contrast well, while AM3_pH5, where $k_{\text{O}_3}^{\text{SO}_2}$ is constant by design, shows similar changes in R_{ws} at all sites.

The increase of η_{DJF} has important implications for the future seasonality of $[\text{SO}_4^{2-}]$. In AM3_pH5, η_{DJF} is lower than η_{JJA} over the 1985–2050 period and the seasonality of $[\text{SO}_4^{2-}]$ is projected to remain similar to present day, with lower $[\text{SO}_4^{2-}]$ in DJF than in JJA. In contrast, η_{DJF} in AM3_BASE is actually simulated to exceed η_{JJA} by 2050, following the increase of $k_{\text{O}_3}^{\text{SO}_2}$ together with the slower removal of SO_2 by deposition in winter than summer. The increase of η_{DJF} contributes to the simulated shift in the seasonality of $[\text{SO}_4^{2-}]$, resulting in higher $[\text{SO}_4^{2-}]$ in winter than in summer ($R_{ws} > 1$) in 2050 at all stations (Figure 4). Figure 5 also shows that $[\text{SO}_4^{2-}]$ (DJF) is projected to remain stable in the coming decades in AM3_BASE, as the increase in the oxidation of SO_2 by O_3 cancels out much of the expected decrease from SO_2 emissions. In contrast, changes in $[\text{SO}_4^{2-}]$ (JJA) reflect more directly the changes in SO_2 emissions, as the increase in the oxidation of SO_2 by H_2O_2 and O_3 is compensated by a decrease of the oxidation of SO_2 by OH (Figure 5).

3.3. Influence of Transition Metals and NH_3 on $[\text{SO}_4^{2-}]$ (DJF)

The analysis of η in the previous section suggests that AM3 low bias in R_{ws} at high $S(\text{SO}_2)$ is associated with a missing oxidation pathway in winter. Several studies have shown that SO_2 can be oxidized by O_2 , either in cloud in the presence of transition metals (TM) [Hoffmann and Jacob, 1984; Martin and Good, 1991] or on aerosol surfaces [Turšič et al., 2003, 2004; Hung and Hoffmann, 2015]. Both of these pathways can operate under acidic conditions and do not exhibit the same titration as H_2O_2 under high SO_2 .

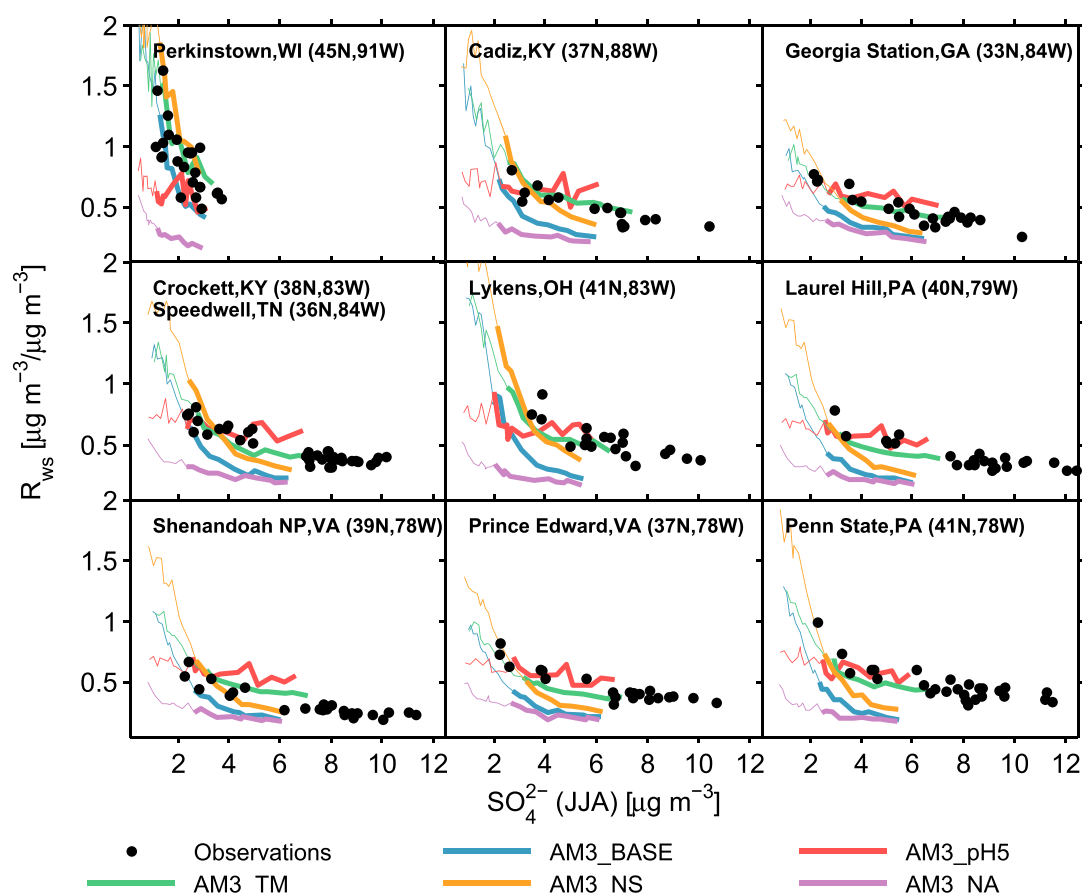


Figure 4. Same as Figure 3 but with different configurations of AM3.

Here we examine the impact of TM chemistry, which is expected to be most important in wintertime in polluted midlatitudes [McCabe *et al.*, 2006; Alexander *et al.*, 2009]. We find that AM3_TM greatly reduces the bias in R_{ws} at high $S(\text{SO}_2)$ (Figure 4). However, over much of the historical period, TM-catalyzed chemistry itself only contributes one third of the additional production of SO_4^{2-} in winter (Figure 5) relative to AM3_BASE. The remaining is from direct emissions of SO_4^{2-} (taken as 3% of anthropogenic SO_2 emissions in our AM3_TM simulation). This suggests that the large uncertainty in the fraction of anthropogenic S emitted as SO_4^{2-} [Textor *et al.*, 2006; Dominguez *et al.*, 2008] may also contribute to biases in R_{ws} at high $S(\text{SO}_2)$. The contribution of TM chemistry increases as $S(\text{SO}_2)$ decreases, which can be attributed to the greater effective solubility of SO_2 at higher pH. In 2050 about 8% of SO_2 is converted to SO_4^{2-} via TM chemistry. However, TM chemistry does not significantly increase the overall conversion of SO_2 into SO_4^{2-} under these conditions ($\eta_{\text{DJF}}(\text{AM3_BASE}) \approx \eta_{\text{DJF}}(\text{AM3_TM})$ at low $S(\text{SO}_2)$).

Our analysis of η shows that changes in cloud pH are essential to understanding the rapid increase of R_{ws} in recent years and its future sensitivity to the continued decline of SO_2 sources. NH_3 plays an important role in setting cloud pH, thereby modulating SO_4^{2-} production by the pH sensitive O_3 pathway [Wells *et al.*, 1997; Redington *et al.*, 2009; Kokkola *et al.*, 2003; Wang *et al.*, 2011; Banzhaf *et al.*, 2012; Megaritis *et al.*, 2013]. Unlike SO_2 (and NO_x), whose emissions from fossil fuel combustion are rapidly declining, anthropogenic emissions of NH_3 (primarily from agriculture) have varied little over the last 30 years [EPA, 2016] and are expected to increase globally as food demand rises. U.S. NH_3 emissions are not regulated, and significant uncertainties remain in their magnitude, spatial distribution, and seasonality [Paulot *et al.*, 2014]. The temporal variations of anthropogenic NH_3 emissions reflect both the seasonality of agricultural activities (e.g., peak in spring from fertilizer application) and the increase of NH_3 volatility with temperature (peak in summer) [Pinder *et al.*, 2006; Skjøth *et al.*, 2011; Paulot *et al.*, 2014]. No seasonality of NH_3 emissions is included in the inventories used by CMIP5 models [Lamarque *et al.*, 2010], leading to an overestimate of wintertime NH_3 emissions (increasing wintertime cloud pH). Figure 5 shows that this neglect of seasonality results in greater oxidation of SO_2 by O_3 in

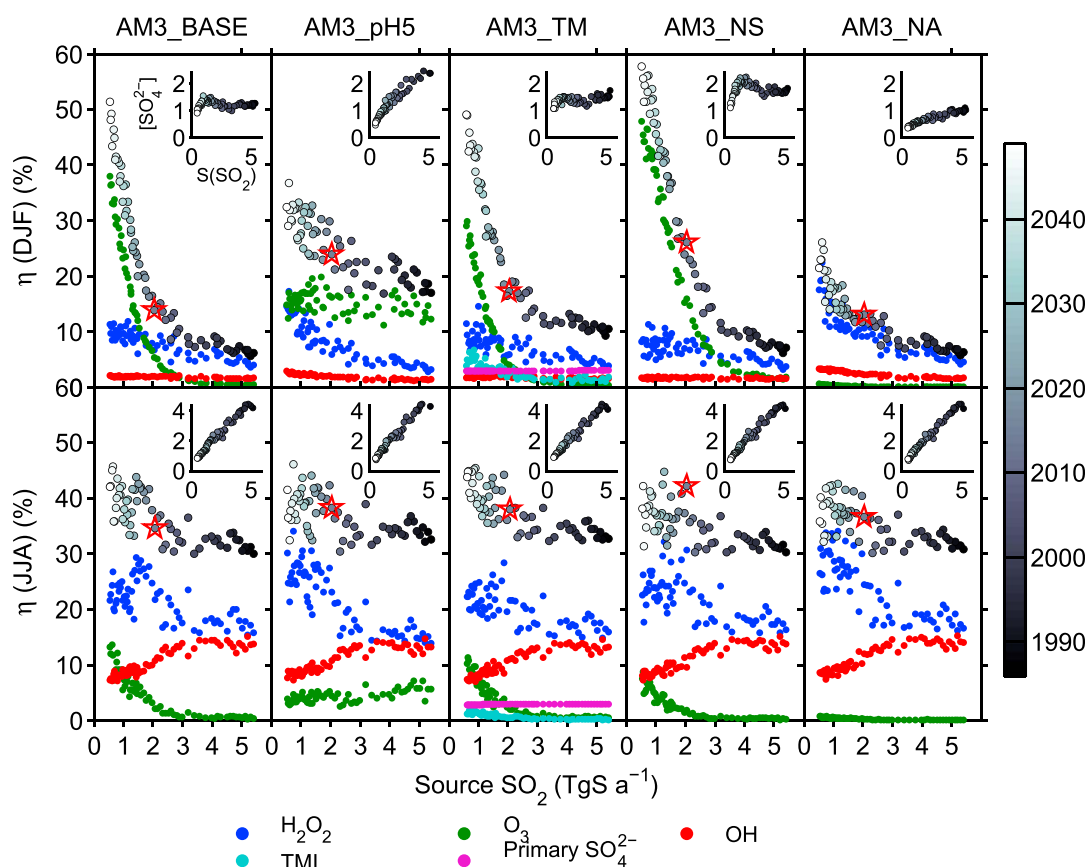


Figure 5. Simulated conversion efficiency (η) of SO_2 to SO_4^{2-} in the Eastern U.S. (dashed region in Figure 2) from 1985 to 2050. Circles are shaded by the simulation year. Year 2015 is indicated by a red star. The simulated change in $[\text{SO}_4^{2-}]$ ($\mu\text{g m}^{-3}$) with decreasing SO_2 emissions ($S(\text{SO}_2)$) in the Eastern U.S. is shown in the insets. Colors indicate the contribution of the different pathways to SO_4^{2-} production.

winter at a given $S(\text{SO}_2)$ in AM3_NS than in AM3_BASE, such that simulated $[\text{SO}_4^{2-}]$ (DJF) over the Eastern U.S. in AM3_NS in 2045 is similar to that of AM3_BASE in 2015. Conversely, when anthropogenic emissions of NH_3 are neglected entirely, clouds remain too acidic for the oxidation of SO_2 by O_3 to be important even in 2050 (Figure 5). Similar to AM3_pH5, the change in η_{DJF} (and thus R_{ws}) is then almost solely driven by diminishing titration of H_2O_2 , resulting in a lower sensitivity of R_{ws} to $S(\text{SO}_2)$. By 2050, simulated R_{ws} can be as much as a factor of 4 lower in AM3_NA than in AM3_BASE in 2050. This shows that agricultural NH_3 emissions modulate the atmospheric S budget and delay the response of $[\text{SO}_4^{2-}]$ (DJF) to SO_2 emissions controls.

4. Conclusions

Observations indicate a marked seasonal contrast in the response of $[\text{SO}_4^{2-}]$ to declining SO_2 emissions with $[\text{SO}_4^{2-}]$ declining more rapidly in summer than in winter. The lack of consistency in simulating this seasonal response by CMIP5 models highlights important uncertainties in the representation of the atmospheric S budget. However, the sources of model biases (e.g., emissions, deposition, and chemistry) are challenging to disentangle. Our study suggests that long-term observations of the relative change of winter to summer $[\text{SO}_4^{2-}]$ in response to SO_2 emission controls can provide a test of the representation of SO_2 chemistry in global models.

Our analysis suggests that the slower decline of $[\text{SO}_4^{2-}]$ in DJF than in JJA is primarily driven by an increase of the photochemical conversion efficiency of SO_2 to SO_4^{2-} in winter. This increase reflects diminishing in-cloud titration of H_2O_2 by SO_2 in the 1990s and faster oxidation of SO_2 by O_3 , promoted by decreasing cloud acidity, from the early 2000s onward. Our model suggests that the winter conversion efficiency of SO_2 to SO_4^{2-} will continue to increase as SO_2 emissions decline, such that SO_4^{2-} (DJF) will decrease much less than SO_2

emissions in the coming decades. These contrasting trends are also projected to reverse the current seasonality of $[\text{SO}_4^{2-}]$, with concentrations becoming higher in winter than in summer. Isotopic measurements [McCabe et al., 2006; Alexander et al., 2009; Harris et al., 2013]) would be especially useful to test whether SO_2 oxidation by O_3 is increasing as suggested by AM3.

We showed that $[\text{SO}_4^{2-}]$ (DJF) declines more sharply in response to SO_2 emission reductions in the absence of NH_3 emissions, as cloud pH would remain too low to allow significant oxidation of SO_2 by O_3 . Thus, anthropogenic NH_3 emissions, which are expected to continue to increase in the future, contribute not only directly (via NH_4NO_3) [Pinder et al., 2007; Heald et al., 2012; Paulot and Jacob, 2014] but also indirectly (via increased SO_4^{2-} production) to challenges in improving U.S. winter air quality [Hand et al., 2012a].

Acknowledgments

CASTNET observations and CMIP5 data can be obtained at www.epa.gov/castnet and esgf-index1.ceda.ac.uk/search/cmip5-ceda, respectively. The output of AM3 sensitivity simulations is available upon request (Fabien.Paulot@noaa.gov). We acknowledge the World Climate Research Programme's Working Group on Coupled Modelling, which is responsible for CMIP, and we thank the climate modeling groups (listed in Table S3 of this paper) for producing and making available their model output. For CMIP the U.S. Department of Energy's Program for Climate Model Diagnosis and Intercomparison provides coordinating support and led development of software infrastructure in partnership with the Global Organization for Earth System Science Portals. We thank Vashali Naik, Paul Ginoux, and Erik Mason for their help. This study was supported by NOAA Climate Program Office's Atmospheric Chemistry, Carbon Cycle, and Climate program.

References

- Alexander, B., R. J. Park, D. J. Jacob, and S. Gong (2009), Transition metal-catalyzed oxidation of atmospheric sulfur: Global implications for the sulfur budget, *J. Geophys. Res.*, *114*, D02309, doi:10.1029/2008JD010486.
- Ames, R. B., and W. C. Malm (2001), Comparison of sulfate and nitrate particle mass concentrations measured by IMPROVE and the CDN, *Atmos. Environ.*, *35*, 905–916.
- Banzhaf, S., M. Schaap, A. Kerschbaumer, E. Reimer, R. Stern, E. van der Swaluw, and P. Bultjes (2012), Implementation and evaluation of pH-dependent cloud chemistry and wet deposition in the chemical transport model REM-Calgrid, *Atmos. Environ.*, *49*, 378–390.
- Banzhaf, S., et al. (2015), Dynamic model evaluation for secondary inorganic aerosol and its precursors over Europe between 1990 and 2009, *Geosci. Model Dev.*, *8*, 1047–1070.
- Barth, M. C., P. J. Rasch, J. T. Kiehl, C. M. Benkovitz, and S. E. Schwartz (2000), Sulfur chemistry in the National Center for Atmospheric Research Community Climate Model: Description, evaluation, features, and sensitivity to aqueous chemistry, *J. Geophys. Res.*, *105*, 1387–1415.
- Bellouin, N., J. Rae, A. Jones, C. Johnson, J. Haywood, and O. Boucher (2011), Aerosol forcing in the Climate Model Intercomparison Project (CMIP5) simulations by HadGEM2-ES and the role of ammonium nitrate, *J. Geophys. Res.*, *116*, D20206, doi:10.1029/2011JD016074.
- Bentsen, M., et al. (2013), The Norwegian Earth System Model, NorESM1-M. Part 1: Description and basic evaluation of the physical climate, *Geosci. Model Dev.*, *6*, 687–720.
- Berglen, T. F., T. K. Berntsen, I. S. A. Isaksen, and J. K. Sundet (2004), A global model of the coupled sulfur/oxidant chemistry in the troposphere: The sulfur cycle, *J. Geophys. Res.*, *109*, D19310, doi:10.1029/2003JD003948.
- Chin, M., D. J. Jacob, G. M. Gardner, M. S. Foreman-Fowler, P. A. Spiro, and D. L. Savoie (1996), A global three-dimensional model of tropospheric sulfate, *J. Geophys. Res.*, *101*, 18,667–18,690.
- Chin, M., R. B. Rood, S.-J. Lin, J.-F. Müller, and A. M. Thompson (2000), Atmospheric sulfur cycle simulated in the global model GOCART: Model description and global properties, *J. Geophys. Res.*, *105*, 24,671–24,687.
- Collins, M., et al. (2013), *Long-Term Climate Change: Projections, Commitments and Irreversibility*, book section 12, pp. 1029–1136, Cambridge Univ. Press, Cambridge, U. K., and New York.
- Collins, W. J., et al. (2011), Development and evaluation of an Earth-System model—HadGEM2, *Geosci. Model Dev.*, *4*, 1051–1075.
- Dix, M., et al. (2013), The ACCESS coupled model: Documentation of core CMIP5 simulations and initial results, *Aust. Meteorol. Oceanogr. J.*, *63*, 83–99.
- Dominguez, G., T. Jackson, L. Brothers, B. Barnett, B. Nguyen, and M. H. Thiemens (2008), Discovery and measurement of an isotopically distinct source of sulfate in Earth's atmosphere, *Proc. Natl. Acad. Sci. U.S.A.*, *105*, 12,769–12,773.
- Donner, L. J., et al. (2011), The dynamical core, physical parameterizations, and basic simulation characteristics of the atmospheric component AM3 of the GFDL global coupled model CM3, *J. Clim.*, *24*, 3484–3519.
- Dufresne, J.-L., et al. (2013), Climate change projections using the IPSL-CM5 Earth System Model: From CMIP3 to CMIP5, *Clim. Dyn.*, *40*, 2123–2165.
- Ervens, B. (2015), Modeling the processing of aerosol and trace gases in clouds and fogs, *Chem. Rev.*, *115*, 4157–4198.
- Flato, G., et al. (2013), *Evaluation of Climate Models*, book section 9, pp. 741–866, Cambridge Univ. Press, Cambridge, U. K., and New York.
- Garmo, Ø. A., et al. (2014), Trends in surface water chemistry in acidified areas in Europe and North America from 1990 to 2008, *Water Air Soil Pollut.*, *225*, 1–14.
- Griffies, S. M., et al. (2011), The GFDL CM3 coupled climate model: Characteristics of the ocean and sea ice simulations, *J. Clim.*, *24*, 3520–3544.
- Hand, J. L., K. Gebhart, B. Schichtel, and W. Malm (2012a), Increasing trends in wintertime particulate sulfate and nitrate ion concentrations in the great plains of the United States (2000–2010), *Atmos. Environ.*, *55*, 107–110.
- Hand, J. L., B. A. Schichtel, W. C. Malm, and M. L. Pitchford (2012b), Particulate sulfate ion concentration and SO_2 emission trends in the United States from the early 1990s through 2010, *Atmos. Chem. Phys.*, *12*, 10,353–10,365.
- Hand, J. L., B. A. Schichtel, W. C. Malm, S. Copeland, J. V. Molenaar, N. Frank, and M. Pitchford (2014), Widespread reductions in haze across the United States from the early 1990s through 2011, *Atmos. Environ.*, *94*, 671–679.
- Harris, E., et al. (2013), Enhanced role of transition metal ion catalysis during in-cloud oxidation of SO_2 , *Science*, *340*, 727–730.
- Heald, C. L., et al. (2012), Atmospheric ammonia and particulate inorganic nitrogen over the United States, *Atmos. Chem. Phys.*, *12*, 10,295–10,312.
- Hoffmann, M. R., and D. J. Jacob (1984), *Kinetics and Mechanisms of the Catalytic Oxidation of Dissolved Sulfur Dioxide in Aqueous Solution: An Application to Nighttime Fog Water Chemistry*, vol. 3, pp. 101–172, Butterworth Publ., Boston, Mass.
- Hung, H.-M., and M. R. Hoffmann (2015), Oxidation of gas-phase SO_2 on the surfaces of acidic microdroplets: Implications for sulfate and sulfate radical anion formation in the atmospheric liquid phase, *Environ. Sci. Technol.*, *49*, 13,768–13,776.
- Janssens-Maenhout, G., et al. (2015), HTAP_v2.2: A mosaic of regional and global emission grid maps for 2008 and 2010 to study hemispheric transport of air pollution, *Atmos. Chem. Phys.*, *15*, 11,411–11,432.
- John, J. G., A. M. Fiore, V. Naik, L. W. Horowitz, and J. P. Dunne (2012), Climate versus emission drivers of methane lifetime against loss by tropospheric OH from 1860–2100, *Atmos. Chem. Phys.*, *12*, 12,021–12,036.
- Kalnay, E., et al. (1996), The NCEP/NCAR 40-year reanalysis project, *Bull. Am. Meteorol. Soc.*, *77*, 437–471.
- Kirkevåg, A., et al. (2013), Aerosol-climate interactions in the Norwegian Earth System Model—NorESM1-M, *Geosci. Model Dev.*, *6*, 207–244.

- Koch, D., D. Jacob, I. Tegen, D. Rind, and M. Chin (1999), Tropospheric sulfur simulation and sulfate direct radiative forcing in the Goddard Institute for Space Studies general circulation model, *J. Geophys. Res.*, *104*, 23,799–23,822.
- Kokkola, H., S. Romakkaniemi, and A. Laaksonen (2003), On the formation of radiation fogs under heavily polluted conditions, *Atmos. Chem. Phys.*, *3*, 581–589.
- Lamarque, J.-F., G. Kyle, M. Meinshausen, K. Riahi, S. Smith, D. van Vuuren, A. Conley, and F. Vitt (2011), Global and regional evolution of short-lived radiatively-active gases and aerosols in the representative concentration pathways, *Clim. Change*, *109*, 191–212, doi:10.1007/s10584-011-0155-0.
- Lamarque, J.-F., et al. (2010), Historical (1850–2000) gridded anthropogenic and biomass burning emissions of reactive gases and aerosols: Methodology and application, *Atmos. Chem. Phys.*, *10*, 7017–7039.
- Lin, M., et al. (2012), Transport of Asian ozone pollution into surface air over the western United States in spring, *J. Geophys. Res.*, *117*, D00V07, doi:10.1029/2011JD016961.
- Lohmann, U., K. von Salzen, N. McFarlane, H. G. Leighton, and J. Feichter (1999), Tropospheric sulfur cycle in the Canadian general circulation model, *J. Geophys. Res.*, *104*, 26,833–26,858.
- Malm, W. C., B. A. Schichtel, R. B. Ames, and K. A. Gebhart (2002), A 10-year spatial and temporal trend of sulfate across the United States, *J. Geophys. Res.*, *107*, 4627, doi:10.1029/2002JD002107.
- Manktelow, P. T., G. W. Mann, K. S. Carslaw, D. V. Spracklen, and M. P. Chipperfield (2007), Regional and global trends in sulfate aerosol since the 1980s, *Geophys. Res. Lett.*, *34*, L14803, doi:10.1029/2006GL028668.
- Martin, L. R., and T. W. Good (1991), Catalyzed oxidation of sulfur dioxide in solution: The iron-manganese synergism, *Atmos. Environ.*, *25*, 2395–2399.
- McCabe, J. R., J. Savarino, B. Alexander, S. Gong, and M. H. Thiemens (2006), Isotopic constraints on non-photochemical sulfate production in the Arctic winter, *Geophys. Res. Lett.*, *33*, L05810, doi:10.1029/2005GL025164.
- Megaritis, A. G., C. Fountoukis, P. E. Charalampidis, C. Pilinis, and S. N. Pandis (2013), Response of fine particulate matter concentrations to changes of emissions and temperature in Europe, *Atmos. Chem. Phys.*, *13*, 3423–3443.
- Meinshausen, M., et al. (2011), The RCP greenhouse gas concentrations and their extensions from 1765 to 2300, *Clim. Change*, *109*, 213–241, doi:10.1007/s10584-011-0156-z.
- Mueller, S. F. (2003), Seasonal aerosol sulfate trends for selected regions of the United States, *J. Air Waste Manag. Assoc.*, *53*, 168–184.
- Naik, V., L. W. Horowitz, A. M. Fiore, P. Ginoux, J. Mao, A. M. Aghedo, and H. Levy (2013), Impact of preindustrial to present-day changes in short-lived pollutant emissions on atmospheric composition and climate forcing, *J. Geophys. Res. Atmos.*, *118*, 8086–8110.
- Paulot, F., and D. J. Jacob (2014), Hidden cost of U.S. agricultural exports: Particulate matter from ammonia emissions, *Environ. Sci. Technol.*, *48*, 903–908.
- Paulot, F., D. J. Jacob, R. W. Pinder, J. O. Bash, K. Travis, and D. K. Henze (2014), Ammonia emissions in the United States, European Union, and China derived by high-resolution inversion of ammonium wet deposition data: Interpretation with a new agricultural emissions inventory (MASAGE_NH3), *J. Geophys. Res. Atmos.*, *119*, 4343–4364.
- Paulot, F., P. Ginoux, W. F. Cooke, L. J. Donner, S. Fan, M.-Y. Lin, J. Mao, V. Naik, and L. W. Horowitz (2016), Sensitivity of nitrate aerosols to ammonia emissions and to nitrate chemistry: Implications for present and future nitrate optical depth, *Atmos. Chem. Phys.*, *16*, 1459–1477.
- Pinder, R. W., P. J. Adams, S. N. Pandis, and A. B. Gilliland (2006), Temporally resolved ammonia emission inventories: Current estimates, evaluation tools, and measurement needs, *J. Geophys. Res.*, *111*, D16310, doi:10.1029/2005JD006603.
- Pinder, R. W., P. J. Adams, and S. N. Pandis (2007), Ammonia emission controls as a cost-effective strategy for reducing atmospheric particulate matter in the Eastern United States, *Environ. Sci. Technol.*, *41*, 380–386.
- Rayner, N. A., D. E. Parker, E. B. Horton, C. K. Folland, L. V. Alexander, D. P. Rowell, E. C. Kent, and A. Kaplan (2003), Global analyses of sea surface temperature, sea ice, and night marine air temperature since the late nineteenth century, *J. Geophys. Res.*, *108*, 4407, doi:10.1029/2002JD002670.
- Redington, A. L., R. G. Derwent, C. S. Witham, and A. J. Manning (2009), Sensitivity of modelled sulphate and nitrate aerosol to cloud, pH and ammonia emissions, *Atmos. Environ.*, *43*, 3227–3234.
- Rotstayn, L. D., and U. Lohmann (2002), Simulation of the tropospheric sulfur cycle in a global model with a physically based cloud scheme, *J. Geophys. Res.*, *107*, 4592, doi:10.1029/2002JD002128.
- Rotstayn, L. D., S. J. Jeffrey, M. A. Collier, S. M. Dravitzki, A. C. Hirst, J. I. Syktus, and K. K. Wong (2012), Aerosol- and greenhouse gas-induced changes in summer rainfall and circulation in the Australasian region: A study using single-forcing climate simulations, *Atmos. Chem. Phys.*, *12*, 6377–6404.
- Salzen, K. V., et al. (2013), The Canadian fourth generation atmospheric global climate model (CanAM4). Part I: Representation of physical processes, *Atmos. Ocean*, *51*, 104–125.
- Schmidt, G. A., et al. (2006), Present-day atmospheric simulations using GISS ModelE: Comparison to in situ, satellite, and reanalysis data, *J. Clim.*, *19*, 153–192.
- Seinfeld, J. H., and S. N. Pandis (2006), *Atmospheric Chemistry and Physics: From Air Pollution to Climate Change*, Wiley, Hoboken, N. J.
- Shindell, D. T., et al. (2013), Interactive ozone and methane chemistry in GISS-E2 historical and future climate simulations, *Atmos. Chem. Phys.*, *13*, 2653–2689.
- Skjøth, C. A., et al. (2011), Spatial and temporal variations in ammonia emission—A freely accessible model code for Europe, *Atmos. Chem. Phys.*, *11*, 5221–5236.
- Sofen, E. D., B. Alexander, and S. A. Kunasek (2011), The impact of anthropogenic emissions on atmospheric sulfate production pathways, oxidants, and ice core $\Delta^{17}\text{O}(\text{SO}_4^{2-})$, *Atmos. Chem. Phys.*, *11*, 3565–3578.
- Takemura, T., T. Nozawa, S. Emori, T. Y. Nakajima, and T. Nakajima (2005), Simulation of climate response to aerosol direct and indirect effects with aerosol transport-radiation model, *J. Geophys. Res.*, *110*, D02202, doi:10.1029/2004JD005029.
- Tanner, R. L., S. T. Bairai, and S. F. Mueller (2015), Trends in concentrations of atmospheric gaseous and particulate species in rural eastern Tennessee as related to primary emission reductions, *Atmos. Chem. Phys.*, *15*, 9781–9797.
- Taylor, K. E., R. J. Stouffer, and G. A. Meehl (2012), An overview of CMIP5 and the experiment design, *Bull. Am. Meteorol. Soc.*, *93*, 485–498.
- Textor, C., et al. (2006), Analysis and quantification of the diversities of aerosol life cycles within AeroCom, *Atmos. Chem. Phys.*, *6*, 1777–1813.
- Thomson, A. M., et al. (2011), RCP4.5: A pathway for stabilization of radiative forcing by 2100, *Clim. Change*, *109*, 77.
- Turšič, J., A. Berner, M. Veber, M. Bizjak, B. Podkrajšek, and I. Grgič (2003), Sulfate formation on synthetic deposits under haze conditions, *Atmos. Environ.*, *37*, 3509–3516.
- Turšič, J., A. Berner, B. Podkrajšek, and I. Grgič (2004), Influence of ammonia on sulfate formation under haze conditions, *Atmos. Environ.*, *38*, 2789–2795.

- U.S. Environmental Protection Agency (U.S. EPA) (2016), *Air Pollutant Emissions Trends Data*. [Available at <https://www.epa.gov/air-emissions-inventories/air-pollutant-emissions-trends-data>.]
- van Vuuren, D., et al. (2011), The representative concentration pathways: An overview, *Clim. Change*, *109*, 5–31.
- von Salzen, K., H. G. Leighton, P. A. Ariya, L. A. Barrie, S. L. Gong, J.-P. Blanchet, L. Spacek, U. Lohmann, and L. I. Kleinman (2000), Sensitivity of sulphate aerosol size distributions and CCN concentrations over North America to SO_x emissions and H₂O₂ concentrations, *J. Geophys. Res.*, *105*, 9741–9765.
- Wang, S., J. Xing, C. Jang, Y. Zhu, J. S. Fu, and J. Hao (2011), Impact assessment of ammonia emissions on inorganic aerosols in east China using response surface modeling technique, *Environ. Sci. Technol.*, *45*, 9293–9300.
- Watanabe, M., et al. (2010), Improved climate simulation by MIROC5: Mean states, variability, and climate sensitivity, *J. Clim.*, *23*, 6312–6335.
- Wells, M., et al. (1997), The reduced nitrogen budget of an orographic cloud, *Atmos. Environ.*, *31*, 2599–2614.
- Yukimoto, S., et al. (2012), A new global climate model of the Meteorological Research Institute: MRI-CGCM3—Model description and basic performance, *J. Meteorol. Soc. Jpn. Ser. II*, *90A*, 23–64.